J Math Chem (2012) 50:394–409
DOI 10.1007/s10910-011-9918-0

ORIGINAL PAPER

Design for an asymmetrical cyclic neutron activation process for determining fluorite grade in fluorspar concentrate

T. Alonso-Sánchez · M. A. Rey-Ronco · M. P. Castro-García · F. J. Carnero-Rodríguez

Received: 12 September 2011 / Accepted: 21 September 2011 / Published online: 5 October 2011

Abstract Conventional neutron activation procedures rely on cycles of equal length to test samples of fluorspar concentrate. This paper proposes a new procedure using "asymmetrical" cycles, in which the duration of the first cycle is different from that of the subsequent activation cycles, which are conducted once the radioactive concentration of the element of interest has been partly reduced through radioactive decay. A comparison is made between the two procedures, and the advantages of the new technique over the conventional one are examined.

Keywords Neutron activation · Cyclic · Symmetrical · Asymmetrical

1 Introduction

An important method for determining which elements are present in a sample is nuclear activation analysis (NAA), a process that works by irradiating the material under study, and then measuring the neutron irradiation of the radionuclides which are directly or indirectly formed [1]. This measurement process is normally subdivided

T. Alonso-Sánchez · M. P. Castro-García (✉) · F. J. Carnero-Rodríguez
Departamento de Explotación y Prospección de Minas, Universidad de Oviedo, Oviedo, Spain
e-mail: castromaria@uniovi.es

T. Alonso-Sánchez
e-mail: tjalonso@uniovi.es

F. J. Carnero-Rodríguez
e-mail: UO168688@uniovi.es

M. A. Rey-Ronco
Departamento de Energía, Universidad de Oviedo, Oviedo, Spain
e-mail: rey@uniovi.es

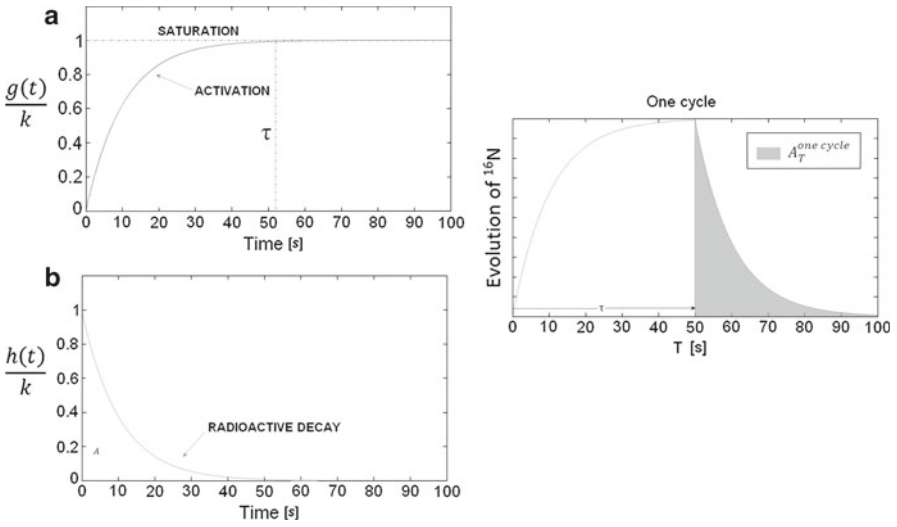

Fig. 1 Radioactive activation and decay in one activation cycle. (Note that the y-axis expresses $\frac{\mathbf{g(t)}}{\mathbf{k}}$ and $\frac{\mathbf{h(t)}}{\mathbf{k}}$

into two distinct phases: first, the sample is irradiated, and second, the induced activity is counted.

While there are different types of neutron activation methods in use, any NAA process must necessarily involve a sample, a neutron source, a gamma ray detector and, of course, a deep understanding of the reactions that take place when the material in question is exposed to neutrons.

The basic difference between the different NAA methods is the moment at which the gamma rays are detected. Thus we have:

- Prompt Gamma-Ray Neutron Activation Analysis (PGNAA), in which the measurement is taken during radiation, and
- Delayed Gamma-Ray Neutron Activation Analysis (DGNAA), in which the measurements are taken based on the radioactive element's decay emissions.

The most widely used of these two methods is DGNAA [2–6], which works as follows:

A sample is irradiated (activation phase), during which time a given element in the sample is exposed to neutrons over a period of time t, giving rise to a new element. If this product is radioactive, its concentration increases over time according to the exponential function $g\,(t) = k \cdot \left(1 - \mathrm{e}^{-\lambda \cdot t}\right)$ (shown in Fig. 1a). In the equation, $\lambda = \frac{\ln(2)}{T_{1/2}}$, where $T_{1/2}$ is the half-life of the product of the reaction, and k is a parameter that depends on several factors, among them the concentration in the sample of the element that produced the radioactive reaction, the type and intensity of the neutron source, the cross-section of the reaction of interest, and the spatial arrangement of the components. When τ reaches a large enough value, $\mathrm{e}^{-\lambda\tau} \rightarrow 0$, a state called "saturation" is reached, i.e. the concentration of the radioactive product stabilizes.

Once the total activation time τ is complete, the sample is removed from the neutron source. Ideally this would take place immediately, but in practice there is usually a short delay as the sample is physically transferred.

Over the next phase, called the "counting time," the spectrum of the gamma rays emitted during the decay of the nuclear reaction are recorded. For any given moment during the counting time, the spectrum records the intensity of the gamma ray radiation. Afterwards, this spectrum is analyzed in two ways. First, the nature of the radioactive product can be determined based on the magnitude of the energy emitted. Second, the concentration of the radioactive element can be determined based on the intensity of the radiation for a given energy reading, expressed in "cps" (counts per second).

The concentration of the radioactive product decays with time, expressed by the equation $h(t) = k \cdot \left(1 - e^{-\lambda \cdot \tau}\right) \cdot e^{-\lambda \cdot (t-\tau)}$ (Fig. 1b). What the detector does is record the cumulative gamma ray spectra over a given period of time, and thus, for any given energy interval, this cumulative reading is equal to the value of the integral of the above function during this period. (Area A of Fig. 1).

The innovation proposed by this research team is to use a single-cycle NAA method for analyzing the fluorite content in a sample of fluorspar concentrate [7,8], an approach that the team has shown to be viable.

In our method, neutrons from an isotopic Americium–Beryllium neutron source are used to irradiate a sample of fluorspar concentrate, which gives rise to hundreds of nuclear reactions. During the ensuing counting time, a NaI(T1) detector is used to record the spectrum of the gamma rays emitted by the radiation's products. The most important reaction for the scope of this study is ^{19}F(n,α)N^{16}, and so it is important to mention that ^{16}N is a radioactive element that is only brought into existence by nuclear reactions, and whose most important characteristics are:

- a half-life, $T_{1/2}$, of 7.13 s [9],
- the emission of high-energy gamma rays of around 7,000 keV, which do not interfere with the energy emitted by other radioactive elements produced in the sample during neutron bombardment [10],
- a highly effective cross-section or probability of occurrence in the energy range of the isotopic source used (between 3 and 10 MeV).

The team was able to determine that all fluorine (F) present in the sample came only from fluorite, and that all the ^{16}N that was produced came solely from the above reaction. This indicates that there is a direct relationship between the fluorite grade in the mineral concentrate and the ^{16}N found by the detector during the decay phase at an energy interval of around 7,000 keV. The name of this reading is $A_T^{one\ cycle}$, which refers to the area recorded by the detector in the energy interval corresponding to ^{16}N, during an activation and counting process equal to T, with just one activation. According to these studies, the area A is related to the fluorite grade in the sample (Fig. 2).

It was found that for a given total experimental time T, the maximum value of $A_T^{one\ cycle}$ occurs when the activation and counting times are equal to $T/2$.

While a very high correlation coefficient was found between the fluorite content of a fluorspar sample and the area of $A_T^{one\ cycle}$, so little ^{16}N is produced during irradiation in an activation cycle, that for this energy interval the detector recorded very few counts. We are currently trying to use the neutron source itself as a means of increasing

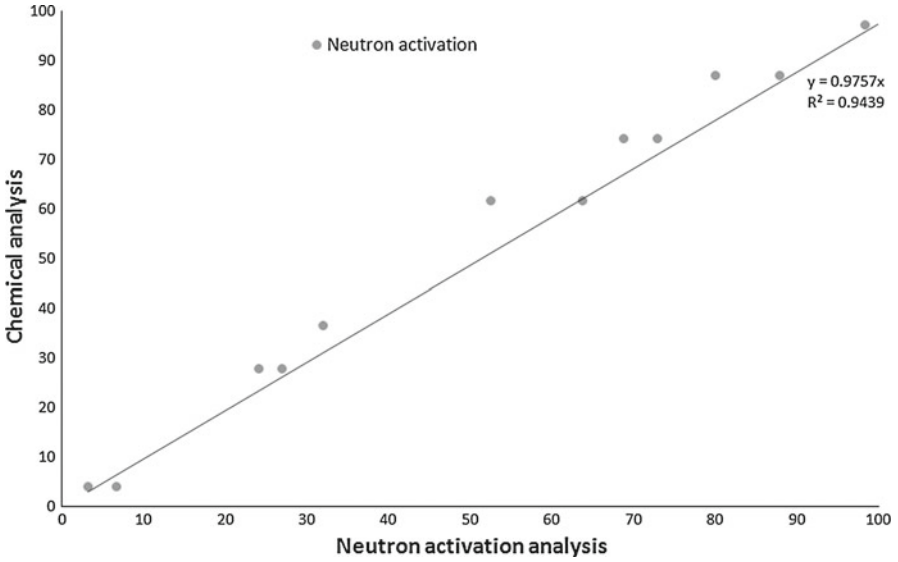

Fig. 2 Comparison between chemical analysis and neutron activation

the intensity of the counts recorded by the detector, in hopes of improving the results' resolution.

Along these same lines, we decided to try using the cyclic activation technique as a means of increasing the area's value. The cyclic process, which has already been described by several authors [11,12], consists of first irradiating the sample for a short period of time, and then, after a short delay, counting the radiation emitted by the sample. After this the sample is irradiated once again, and the whole process is repeated for a number of cycles n [13], hence the name.

In terms of the concentration of ^{16}N, the cyclic activation model works as follows. If in the first activation 70% of the concentration of ^{16}N at saturation is reached, then at the outset of the second activation cycle, the amount of ^{16}N will have dropped to around 2%, as shown in Fig. 3. Once the second activation phase begins, new ^{16}N begins to form. At the end of the second activation the amount of ^{16}N left over from the first activation is around 6% of saturation, giving us a total of 76% of saturation, since the amount of new ^{16}N produced in the second activation is essentially the same as that produced in the first (in this case 70%). The third and subsequent cycles are likewise similar to the second in this respect. The method which relies on this type of cycles has thus been referred to as "symmetrical cyclic activation."

The following parameters specific to cyclic activation were defined for each total process duration T: activation time and counting time for each phase in a cycle, along with the number of cycles n. In addition, optimum values were chosen in order to maximize the detector response. Here the detector response is referred to as $A_T^{n\,cycles}(s)$.

Based on this work, the optimum number of cycles, n_{op}, was determined for various experimental times, in order to maximize the detector response for radiation from ^{16}N [14]. Furthermore, it was concluded that the activation and counting times in each cycle should be equal, and should have a value of $\tau_{op} = \frac{T}{2 \cdot n}$.

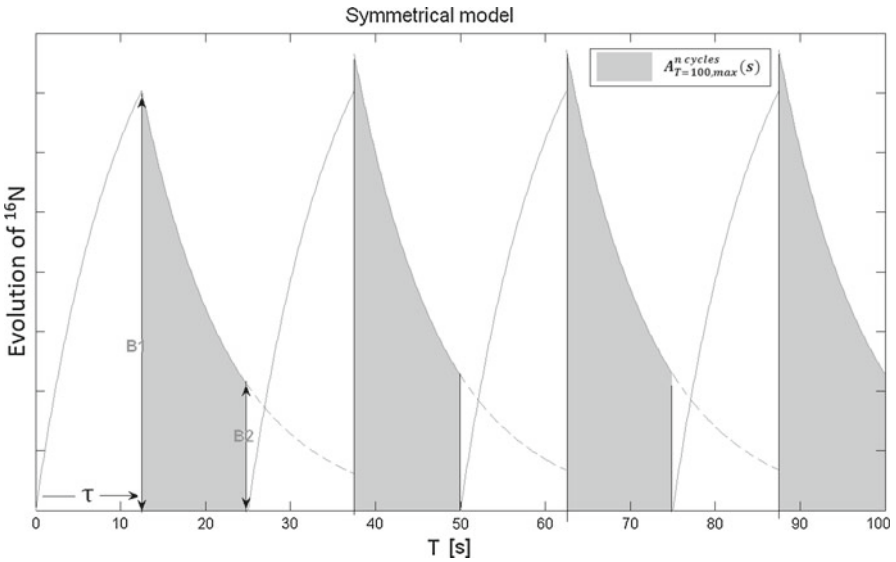

Fig. 3 Symmetrical cyclic activation

The results of these trials are shown in Fig. 4. The optimum number of cycles for an experimental time of $T = 200$ s is eight, and the duration of each phase is $\tau_{op} = \frac{T}{2 \cdot n} = \frac{200}{2 \cdot 8} = 12.5$ s.

The maximum area for this situation is given by substituting $T = 200$ in the following equation, which corresponds to the line in Fig. 4:

$$A^{*n\ cycles}_{max,T} = 0.0199 \cdot T - 0.0221 \tag{1}$$

Which gives us $A^{*n\ cycles}_{max,T} = 3.9579$.

2 Analysis of the asymmetrical cyclic process

Following this work with the symmetrical cyclic method, we devised another type of cycle, which we have called "asymmetrical," in hopes of better detecting fluorite. In this section we will explain how this new method works, and analyze whether it is indeed more effective than the symmetrical cycle.

The process consists of a first activation cycle up to a given concentration of ^{16}N(B_1), followed by a decay cycle down to a lower concentration of ^{16}N(B_2), which is still significantly high, and then repeating the activation and decay cycles within the limits of B_1 and B_2, as can be seen in Fig. 5.

The goal of this process is to increase the number of cycles and record higher values for the area under the decay curve, while disregarding the curve's tail. In order to obtain the maximum area , $A^{n\ cycles}_{T}(a)$ for experiment time T, it is necessary to optimize the activation and counting times. Once this has been done, it can be determined whether

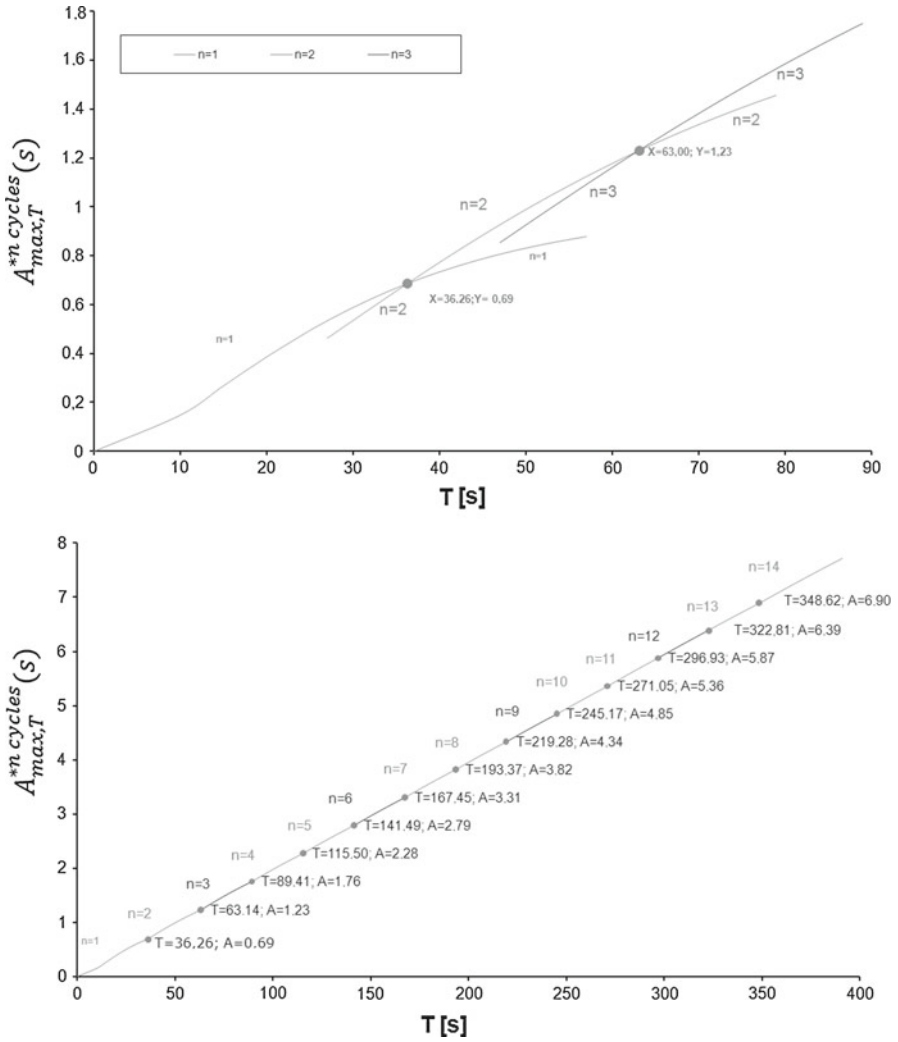

Fig. 4 Relationship between experiment time T, and number of cycles n with respect to $A^{*n\ cycles}_{max,T}$, following Rey–Ronco [14]

or not the asymmetrical approach constitutes an improvement over the conventional symmetrical cyclic activation , $A^{n\,cycles}_{T}(s)$.

Figure 5 shows the variation in the concentration of a radioactive element over time during an asymmetrical cyclic activation process, as defined above.

According to the initial hypotheses:

$$B_1 = k \cdot \left(1 - \mathrm{e}^{-\lambda \cdot (ta + tx)}\right) \tag{2}$$

$$B_2 = B_1 \cdot \mathrm{e}^{-\lambda \cdot tl} \tag{3}$$

$$B_3 = k \cdot (1 - \mathrm{e}^{-\lambda \cdot ta}) \tag{4}$$

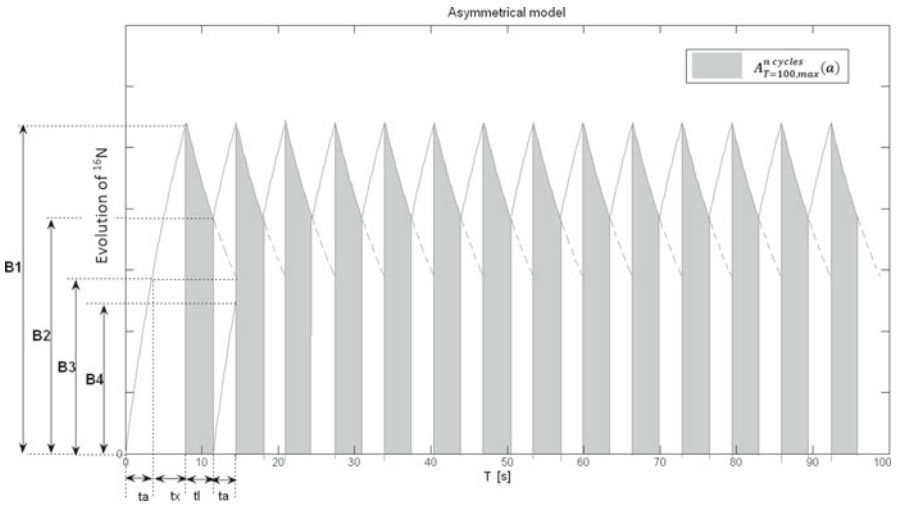

Fig. 5 Representation of the activation-decay cycles in the asymmetrical model. The *grey* sections represent the area of $A_T^{*n\ cycles}(s) = A_T^{n\ cycles}(s) \cdot \frac{\lambda}{k}$ for experiment time $T = 100$ s

$$B_4 = B_1 \cdot \mathrm{e}^{-\lambda \cdot (tl + ta)} \tag{5}$$

In Fig. 5 the parameter B_1 represents the maximum concentration of ^{16}N, and the area marked $A_T^{*n\ cycles}(a)$ in grey represents the measurement or detector response of gamma rays for the total experimental time T and for n cycles. Based on Fig. 5, it is clear that:

$$B_1 = B_3 + B_4 \tag{6}$$

The area of each activation and counting cycle is expressed as:

$$A_T^{n\ cycles}(a) = n \cdot \int_0^{t_l} k \cdot \left(1 - \mathrm{e}^{-\lambda \cdot (t_a + t_x)}\right) \cdot \mathrm{e}^{-\lambda \cdot t} dt \tag{7}$$

Which can be reduced to:

$$A_T^{n\ cycles}(a) = n \cdot \frac{k}{\lambda} \cdot \left(1 - \mathrm{e}^{-\lambda \cdot (t_a + t_x)}\right) \cdot [1 - \mathrm{e}^{-\lambda \cdot t_l}] \tag{8}$$

By making $A_T^{*n\ cycles}(a) = A_T^{n\ cycles}(a) \cdot \frac{\lambda}{k}$ in the above expression, the parameters λ and k can be avoided, as they are constant factors that depend on each individual sample, on the decay characteristics of ^{16}N, or on the instruments being used, and as such have no bearing on maximizing the area:

$$A_T^{*n\ cycles}(a) = n \cdot \left(1 - \mathrm{e}^{-\lambda \cdot (t_a + t_x)}\right) \cdot [1 - \mathrm{e}^{-\lambda \cdot t_l}] \tag{9}$$

2.1 Maximization of the area function $A_T^{*n\ cycles}(a)$

In order to optimize the asymmetrical cyclic activation process, one must determine the number of cycles, n, and the times t_a, t_x, and t_l for a given experimental time T that will maximize the function $A_T^{*n\ cycles}(a)$.

2.1.1 Finding a relationship between variables

By substituting expressions [2,4] y [5] for the terms in Equation [6], we get:

$$k \cdot \left(1-\mathrm{e}^{-\lambda\cdot(t_a+t_x)}\right) = k \cdot \left(1-\mathrm{e}^{-\lambda\cdot t_a}\right) + k \cdot \left(1-\mathrm{e}^{-\lambda\cdot(t_a+t_x)}\right) \cdot \mathrm{e}^{-\lambda\cdot(t_l+t_a)} \tag{10}$$

From which we can deduce that:

$$\mathrm{e}^{-\lambda\cdot(t_a+t_x)} = \frac{k \cdot \left(1-\mathrm{e}^{-\lambda\cdot t_a}\right) - \mathrm{k} + \mathrm{k} \cdot \mathrm{e}^{-\lambda\cdot(t_l+t_a)}}{-k + k \cdot \mathrm{e}^{-\lambda\cdot(t_l+t_a)}} \tag{11}$$

And,

$$t_x = \frac{\lambda \cdot t_a + ln\left(\frac{\mathrm{e}^{-\lambda\cdot t_a}-\mathrm{e}^{-\lambda\cdot(t_a+t_l)}}{1-\mathrm{e}^{-\lambda\cdot(t_a+t_l)}}\right)}{\lambda} \tag{12}$$

Substituting the values from Equation [11] in Expression [9] and simplifying results in the following expression:

$$A_T^{*n\ cycles}(a) = n \cdot \frac{\left(1-\mathrm{e}^{-\lambda\cdot t_a}\right)\cdot\left(1-\mathrm{e}^{-\lambda\cdot t_l}\right)}{\left(1-\mathrm{e}^{-\lambda\cdot(t_a+t_l)}\right)} \tag{13}$$

Furthermore, it holds that:

$$T = n \cdot (t_l + t_a) + t_x \tag{14}$$

Whereby, if we substitute [12] in [13], we are left with:

$$T = n \cdot (t_l + t_a) + \frac{\lambda \cdot t_a + ln\left(\frac{\mathrm{e}^{-\lambda\cdot t_a}-\mathrm{e}^{-\lambda\cdot(t_a+t_l)}}{1-\mathrm{e}^{-\lambda\cdot(t_a+t_l)}}\right)}{\lambda} \tag{15}$$

2.1.2 Procedure using an algorithm

An algorithm created using Matlab was used to determine, for a given experimental time T and a number of cycles n, the value of $A_T^{*n\ cycles}(a)$, and the parameters t_a, t_l, t_x corresponding to the number of cycles that would maximize $A_T^{*n\ cycles}(a)$. Figure 6 shows the flow chart for this algorithm.

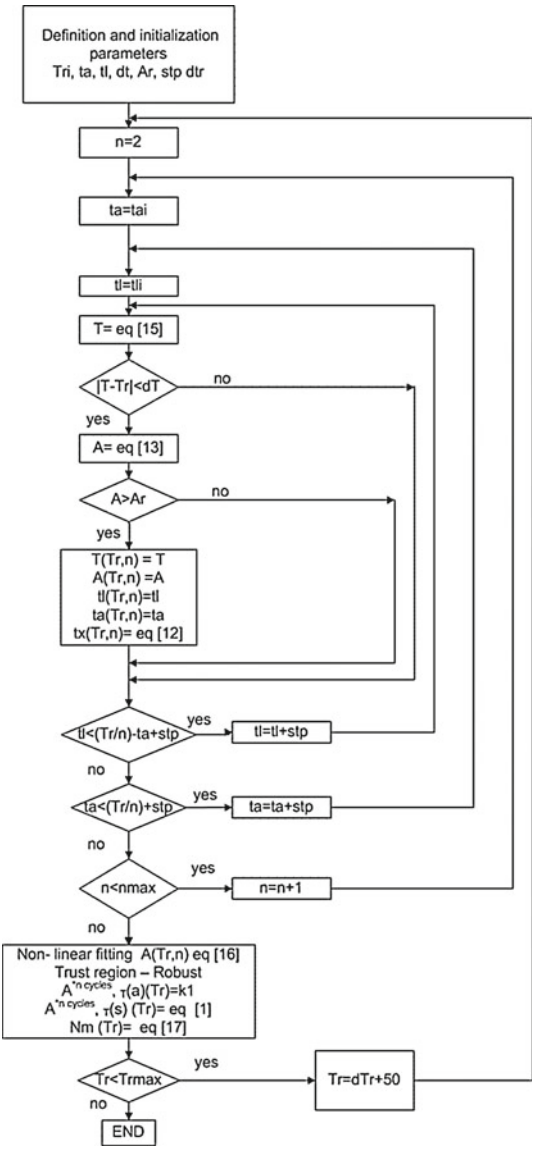

Fig. 6 Flow chart

Table 1 Example of the results of the algorithm

T [s]	n	$A_T^{*n\ cycles}(a)$
200	7	4.159974

Below is an example of the results of this algorithm for the total experimental time $T = 200$ s and $n = 7$ (Table 1).

It was found that for smaller n values, $A_T^{*n\ cycles}(a)$ is lower. This effect was observed for all experiment times. As n increases, $A_T^{*n\ cycles}(a)$ increases until reaching an asymptote for $n = \infty$.

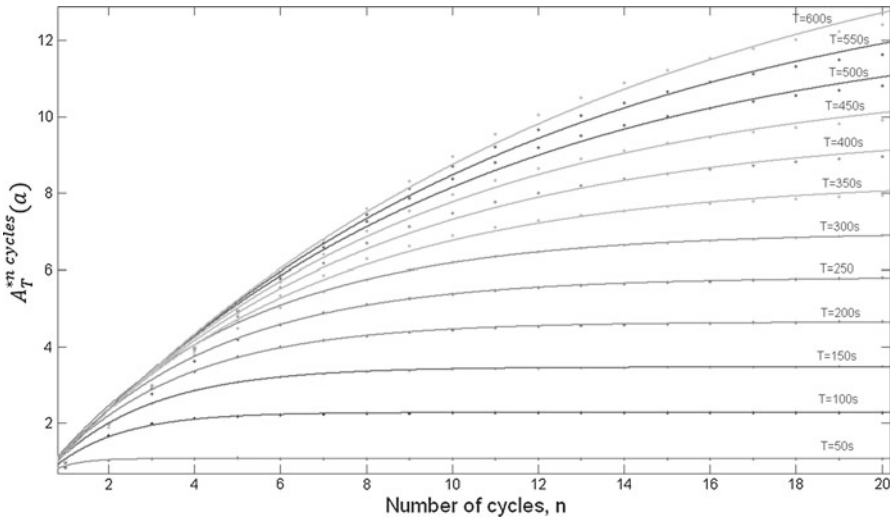

Fig. 7 The curves for the experiment times 50 to 600 s

Subsequently, the results for $A_T^{*n\ cycles}(a) - n$ for $T = 200$ were adjusted to the following curve:

$$A_T^{*n\ cycles}(a) = k1 \cdot (1 - \mathrm{e}^{-k2 \cdot n}) \tag{16}$$

where $k1$ and $k2$ are the adjustment coefficients. $k1$ is the value of the asymptote, and represents the maximum value that could be obtained with asymmetrical cyclic activation.

The results of the above example are as follows (with 95% confidence bounds):

$k1 = 4.646(4.623, 4.669)$
$k2 = 0.3225(0.3152, 0.3298)$

Goodness of fit:

SSE: 0.01992
R_square:0.999
Adjusted R_square: 0.9989
RMSE: 0.03326

This curve is shown in Fig. 7, alongside the curves for the experiment times 50 to 600 s.

3 Comparison of the symmetrical and asymmetrical cycle processes

This section compares the maximum decay area of the symmetrical activation method, $A_{T,max}^{*n\ cycles}(s)$ with that of the asymmetrical method, $A_{T,max}^{*n\ cycles}(a)$, as well as the two methods' activation parameters. Figure 8 shows the number of cycles needed for the

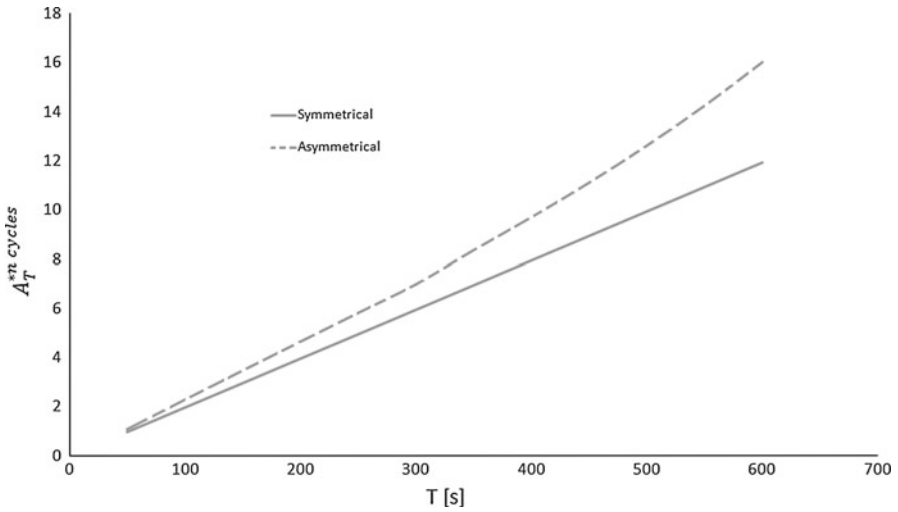

Fig. 8 Comparison between $A_{T,max}^{*n\ cycles}(s)$ and $A_{T,max}^{*n\ cycles}(a)$ for different T

Table 2 Results

T [s]	Symmentrical cycle			Asymmetrical cycle					% improvement
	$A_{T,max}^{*n\ cycles}(s)$	τ	n	$A_{T,max}^{*n\ cycles}(a)$	t_1	t_2	t_x	n_{lim}	
50	0.9729	12.5	2	1.075	12.47	11.3	2.558	2	10.5
100	1.9679	12.5	4	2.28	16.72	16.04	1.82	3	15.9
150	2.9629	12.5	6	3.468	14.93	14.66	2.149	5	17.0
200	3.9579	12.5	8	4.646	16.61	16.43	1.859	6	17.4
250	4.9529	12.5	10	5.816	15.65	15.36	2.017	8	17.4
300	5.9479	12.5	12	6.98	16.71	16.43	1.838	9	17.4
350	6.9429	12.5	14	8.353	16.02	15.63	1.948	11	20.3
400	7.9379	13.33	15	9.69	15.5	15.12	2.039	13	22.1
450	8.9329	13.24	17	11.1	16.04	15.97	1.96	14	24.3
500	9.9279	13.16	19	12.61	16.61	16.6	1.866	15	27.0
550	10.9229	13.1	21	14.24	16.12	16.12	1.949	17	30.4
600	11.9179	13.04	23	16.01	15.16	14.74	2.098	20	34.3

asymmetrical cycle to surpass the symmetrical cycle, a cross-over point that we have called n_{lim}. This value was calculated with the equation:

$$n_{lim} = \frac{1}{k_2} \cdot \ln\left(1 - \frac{0.0199 \cdot T - 0.0221}{k_1}\right) \tag{17}$$

These values are shown in Table 2. This means that, for example, for experimental time $T = 300$, the maximum area that could be obtained by the asymmetrical method

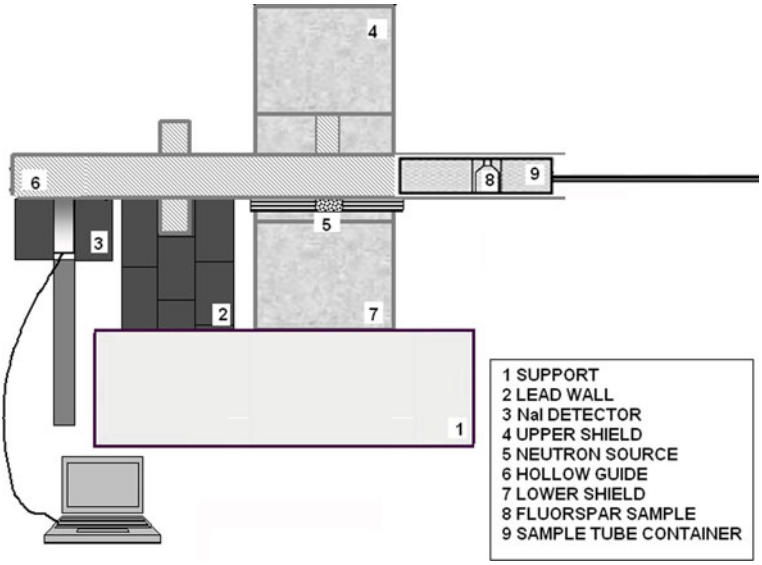

Fig. 9 Prototype 1

is 6.98, compared to 5.9479 for the symmetrical method, which constitutes at 17.4% improvement. Nine cycles are needed for the asymmetrical method to surpass the symmetrical method, with $t_1 = 16.71$, $t_a = 16.43$ and $t_x = 1$.

Figure 8 shows the variation of $A_{T,max}^{*n\,cycles}(a)$ and $A_{T,max}^{*n\,cycles}(s)$ with experimental time. It can be seen how the improvement increases alongside experimental time.

4 Materials and methods

The following section explores the differences between two laboratory systems designed to determine the concentration of fluorite in fluorspar samples by recording gamma radiation from ^{16}N.

4.1 System 1

The team created a prototypical process design which includes the activation system, a detector for measuring the gamma radiation emitted by the fluorspar sample, and a manual mechanism for transferring the sample between these two stations [8], as shown in Fig. 9. The components of this system are as follows:

- The source, which is an alloy of two metals, Americium 241 and Beryllium 9, mounted on a double cylindrical casing of stainless steel. This double capsule is 35 mm long by 30 mm in diameter. The weight of the Americium contained in it is 0.309 g, with 1 Ci of activity. This source emits $3.7 \cdot 10^{10}$ neutrons per second.
- An INA (Tl) detector 2 in. long by 2 in. in diameter
- A Canberra 2700P photomultiplier detector,

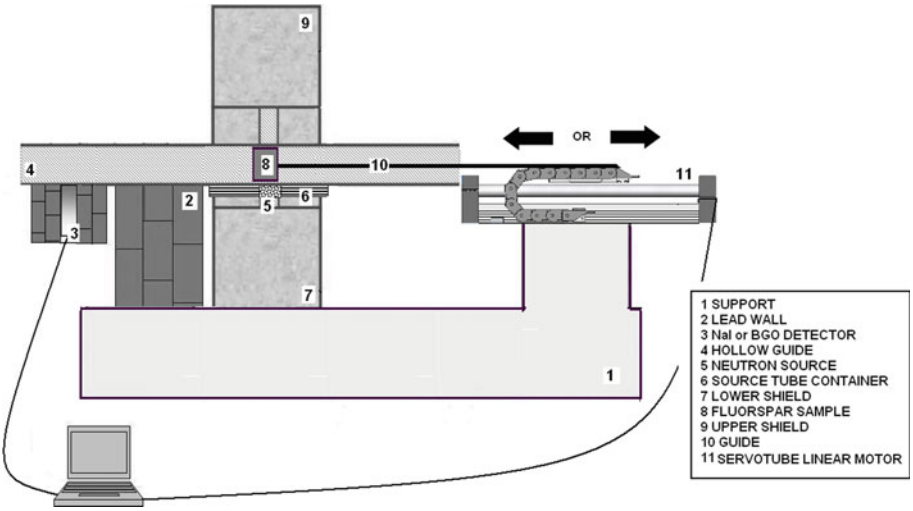

Fig. 10 Prototype 2

- A high tension Ortec 556 source,
- A Canberra 8701 analog/digital converter,
- A Canberra 100 multichannel analyzer, and
- The Software System 100.

Figure 9 shows how the prototype is set up. Given ^{16}N's low half-life of 7.13 s, it is important for the irradiated fluorspar sample to be very near to the reading device. Likewise, it was also necessary to determine the optimal distance between the neutron source and the radiation detector.

The operating procedure includes the following steps:

- Place the sample into position.
- Use the hollow guide to move the sample to the irradiation position, facing the source.
- Expose the sample to irradiation by the neutron source for a period called the "activation" or "irradiation phase."
- Transfer the sample over to the detector
- The detector takes readings of the irradiated sample.

The results obtained with this measurement system showed that neutron activation was indeed a viable method [8]. Furthermore, this initial model was used as the basis for the design and assembly of a second measurement system, in which the sample is transferred between the activation and counting stations with a linear motor.

4.2 System 2

This new system includes an automatic mechanism for transferring the sample, which makes it much easier to carry out both the symmetrical and asymmetrical cycles (Fig. 10). The components of this system are as follows:

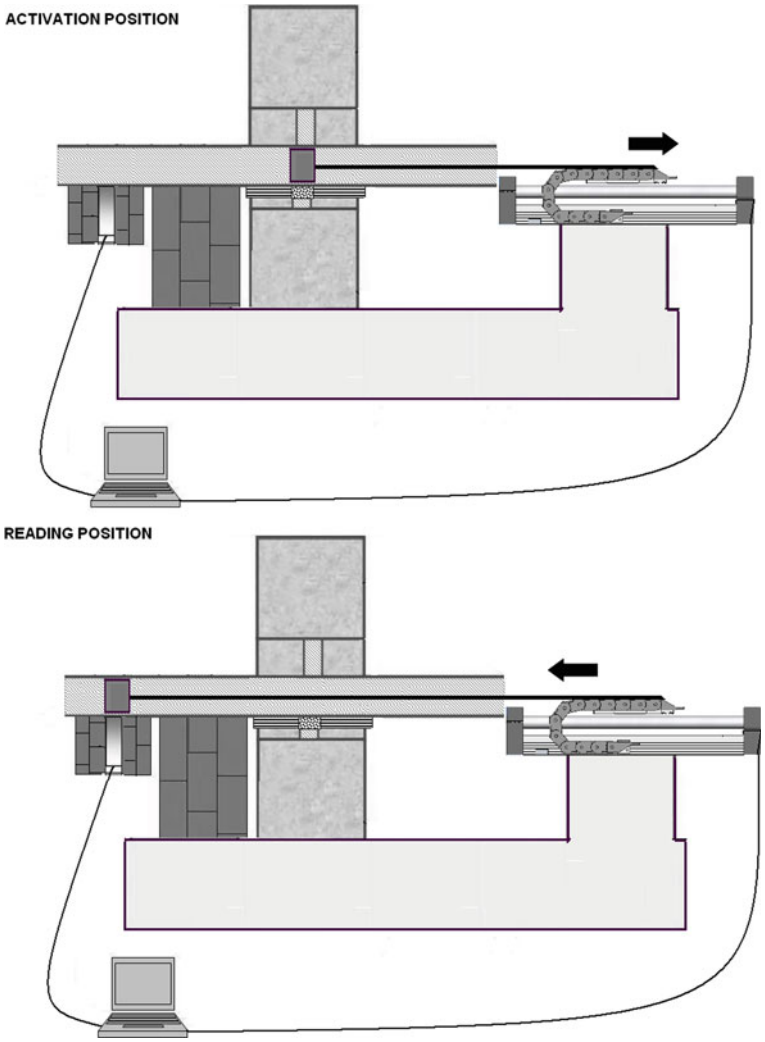

Fig. 11 Activation and counting positions

- The source described above.
- A Canberra INA (Tl) detector, 2 in. long and 2 in. in diameter
- A Canberra BGO detector, 2 in. long and 2 in. in diameter,
- An Osprey Multichannel Analyzer (MCA) and a UniSpec Multichannel Analyzer (MCA) with Canberra Genie 2000 Gamma Acquisition & Analysis Software,
- A Servotube linear motor, 1,130 mm long, 85 mm wide and 93 mm tall, with a maximum velocity of 8.7 m/s.

The operating procedure is similar to previous case and includes the following steps (see Fig. 11):

- Place the sample into position.

- Use the hollow guide to move the sample to the irradiation position, facing the source.
- Expose the sample to irradiation by the neutron source for a period called the "activation" or "irradiation phase."
- Transfer the sample over to the detector; all measurements must be taken within a minimum, fixed and precise span of time.
- The detector takes readings of the irradiated sample.
- Repeat the cycle according to the results of the trial.

5 Results and discussion

This paper discusses a new step forward in neutron activation processes for determining fluorite grade in samples of fluorspar concentrate. Important differences between the conventional symmetrical cyclic activation method and this new "asymmetrical" method are:

- Unlike the symmetrical method, the asymmetrical method's activation and counting times are not equal, although the difference between them is never greater than one second.
- The total duration of an activation-counting cycle is considerably higher in the asymmetrical process than in the symmetrical process.
- The number of cycles, n_{lim} in the asymmetrical process is less than or equal to that of the symmetrical process.
- Time t_x (the extra activation time in the first cycle of the asymmetrical process) is around 2 s, regardless of the experimental time.

Furthermore, it has been seen that for total experiment times of more than 200 s, the asymmetrical cyclic method proposed in this paper constitutes a significant improvement over the conventional, symmetrical cyclic method. At 600 s, for example, the new method offers an improvement on the order of 35%, and this advantage tends to increase alongside the total experimental time. However, for total experimental times of 200 s or less, the new method constitutes only a slight improvement over the conventional method.

It is also worth mentioning that, though shown to be an inadequate neutron source for single-cycle activation processes, a 1 Ci Americium–Beryllium source can in fact be used to determine fluorite grades with superior precision, if used in cyclic activation processes.

Lastly, in practical terms, it is of interest to other researchers to note that any system that is set up for symmetrical cyclic activation can easily accommodate the asymmetrical method proposed in this paper, by simply modifying the software used for transferring the samples.

Acknowledgments The authors would like to thank Mineral Products and Derivatives Company SA (Minersa), the Government of the Principality of Asturias, and the research grant scheme of the University of Oviedo for their collaboration and financial support throughout this study.

References

1. R.H. Filby, Isotopic and nuclear analytical techniques in biological systems: a critical study. Neutron activation analysis. Pure Appl. Chem. **67**(11), 1929–1941 (1995)
2. Y. Maki, T. Nojiri, B.A. Masilungan, The determination of fluorine by cyclic activation analysis method using 241Am-Be neutron source. Radioisotopes **23**, 149–154 (1974)
3. S.E.B. Nonie, K. Randle, A.G. Blackband, Development of a computer-based system for fast neutron cyclic activation analysis. J. Radioanal. Nucl. Chem. **167**, 89–95 (1993)
4. I.W. Croudace, K. Randle, A rapid and non-destructive method of fluorine determination using fast-neutron activation analysis. Chem. Geol. **67**, 165–170 (1988)
5. I.W. Croudace, Fluorine abundances of twenty nine geological and other reference samples using fast-neutron activation analysis. Geostand. Newsl. **127**(2), 127–218 (1993)
6. A. Chatt, K.N. DeSilva, J. Holzbecher, D.C. Stuart, R.E. Tout, D.E. Ryan, Cyclic neutron activation analysis of biological and metallurgical samples. Can. J. Chem. **59**, 1660–1664 (1981)
7. M.A. Rey-Ronco, Desarrollo de un método rápido basado en técnicas de activación neutrónica para la determinación del contenido en flúor de muestras de mineral de fluorita. Universidad de Oviedo. Doctoral thesis. Avalaible from http://www.tesisenred.net/TDR-0802107-133201/index_cs.html (2007)
8. T. Alonso-Sánchez, M.A. Rey-Ronco, M.P. Castro-García, A neutron activation technique for the analysis for fluorine in fluorspar samples. Int. J. Miner. Process. **94**, 1–13 (2011)
9. A. Sonzogni, Nucl. Struct. Decay Data (NuDat). Available from www.nndc.bnl.gov (2011)
10. M. Herman, Experimental nuclear reaction data (EXFOR / CSISRS). Available from www.nndc.bnl.gov (2007)
11. N.M. Spyrou, Cyclic activation analysis a review. J. Radioanal. Chem. **61**, 211–242 (1981)
12. W.W. Givens, W.R Mills, R.L. Caldwell, Cyclic activation analysis. Nucl. Instrum. Methods **80**, 95–103 (1970)
13. X. Hou, in *Cyclic activation analysis*, ed. by R.A. Meyers. Encyclopedia of analytical chemistry (John Wiley & Sons Ltd, Wiley, Chichester, 2000), pp. 12447–12459
14. M.A. Rey-Ronco, T. Alonso-Sánchez, M.P. Castro-García, Mathematical study to improve the sensitivity in the neutron activation analysis of fluorspar. J. Math. Chem. **48**, 165–174 (2010)